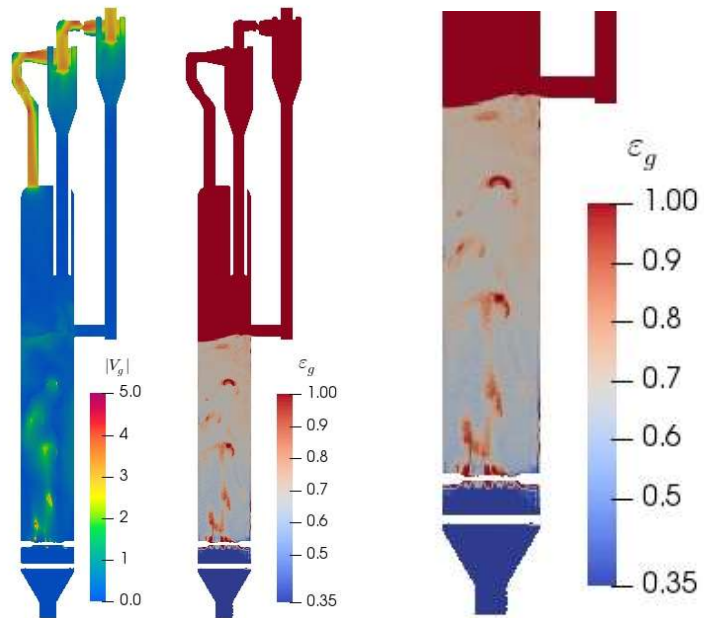




NATIONAL ENERGY TECHNOLOGY LABORATORY



The MFiX Particle-in-Cell Method (MFiX-PIC) Theory Guide

22 May 2020



U.S. DEPARTMENT OF
ENERGY



NATIONAL
ENERGY
TECHNOLOGY
LABORATORY

Office of Fossil Energy

DOE/NETL-2020/2115

Disclaimer

This work was funded by the Department of Energy, National Energy Technology Laboratory, an agency of the United States Government, through a support contract with Leidos Research Support Team (LRST). Neither the United States Government nor any agency thereof, nor any of their employees, nor LRST, nor any of their employees, makes any warranty, expressed or implied, or assumes any legal liability or responsibility for the accuracy, completeness, or usefulness of any information, apparatus, product, or process disclosed, or represents that its use would not infringe privately owned rights. Reference herein to any specific commercial product, process, or service by trade name, trademark, manufacturer, or otherwise, does not necessarily constitute or imply its endorsement, recommendation, or favoring by the United States Government or any agency thereof. The views and opinions of authors expressed herein do not necessarily state or reflect those of the United States Government or any agency thereof.

Cover Illustration: MFiX-PIC simulation of a 3.6 m tall bubbling fluidized bed with fluid catalytic cracking (FCC) particles. The simulation tracks 9.3 M parcels with a statistical weight of 500,000 particles per parcel. The left two images show slices of the velocity and volume fraction fields. The image on the right is a close-up of the volume fraction field.

Suggested Citation: Clarke, M.; Musser, J. *The MFiX Particle-in-Cell Method (MFiX-PIC) Theory Guide*; DOE/NETL-2020/2115; NETL Technical Report Series; U.S. Department of Energy, National Energy Technology Laboratory: Morgantown, WV, 2020; p. 28. DOI: 10.2172/1630414.

The MFiX Particle-in-Cell Method (MFiX-PIC) Theory Guide

Mary Ann Clarke^{1,2} and Jordan Musser¹

¹ **U.S. Department of Energy, National Energy Technology Laboratory, 3610 Collins Ferry Road, Morgantown, WV 26507**

² **U.S. Department of Energy, National Energy Technology Laboratory, Leidos Research Support Team (Battelle), 3610 Collins Ferry Road, Morgantown, WV 26507**

DOE/NETL-2020/2115

22 May 2020

NETL Contacts:

Jordan Musser, Principal Investigator

Jimmy Thornton, Associate Director, Computational Science & Engineering

Bryan Morreale, Executive Director, Research & Innovation Center

This page intentionally left blank.

Table of Contents

EXECUTIVE SUMMARY	1
1. INTRODUCTION.....	2
1.1 OVERVIEW OF MFiX-PIC.....	2
1.2 ASSUMPTIONS/LIMITATIONS	3
1.3 DOCUMENT ORGANIZATION.....	5
2. LAGRANGIAN SOLIDS PHASE MODEL UTILIZED IN PIC.....	6
2.1 OVERVIEW.....	6
2.2 CONSERVATION EQUATIONS.....	6
2.3 PARTICLE-PARTICLE MOMENTUM TRANSFER.....	9
2.4 FLUID-PARCEL MOMENTUM TRANSFER.....	10
2.5 PARCEL-PARCEL HEAT TRANSFER.....	10
2.6 RADIATIVE HEAT TRANSFER.....	10
2.7 FLUID-PARCEL CONVECTIVE HEAT TRANSFER.....	10
2.8 ENERGY TRANSFER ACCOMPANYING MASS TRANSFER	11
2.9 PARCEL PHYSICAL PROPERTIES	11
3. NUMERICAL DETAILS UNIQUE TO MFiX-PIC	13
3.1 OVERVIEW.....	13
3.2 BI-LINEAR INTERPOLATION	13
3.3 BOUNDARY MANAGEMENT	16
4. CONCLUDING REMARKS	18
5. REFERENCES.....	19

List of Figures

Figure 1: Visual concept of particle consolidation to computational parcels by type. (a) A single cell populated with particles. (b) The same single cell after a statistical weight has been applied to each particle type..... 2

Figure 2: Computational PIC parcels are infinitesimal points in space. While the mind easily accepts consolidation of particles into “bigger” parcels, the mathematics acts only on the center of such an imagined parcel..... 4

Figure 3: Typical Bi-linear Interpolation Operator, ***Sxi***..... 13

Figure 4: Parcel (star) in 3-dimensional cell-center view (triangles) used for interpolation. 14

Figure 5: (a) An extension of Figure 4, showing velocity stored at xz-face centers (circles) in the original context of cell-center nodes (triangles).(b) Pulling the new face-centered box out of (a) and applying labels while maintaining the original cell center view of Figure 4..... 15

Acronyms and Abbreviations

Term	Description
CFD	Computational fluid dynamics
DEM	Discrete element method
DOE	Department of Energy
FCC	Fluid catalytic cracking
LRST	Leidos Research Support Team
MFiX	Multiphase Flow with Interphase eXchanges
MP-PIC	Multiphase particle-in-cell
NETL	National Energy Technology Laboratory
PIC	Particle-in-cell
STL	Stereolithographic CAD file
TFM	Two fluid model
VTK	Visualization ToolKit file format

Latin Symbols

Term	Description
A_m	Discrete particle phase acceleration
A_s	Particle surface area
C_p	Parcel specific heat
C_{pm}	m^{th} phase specific heat
D_m	Drag coefficient for solids phase m
g_i	Gravity body force in i^{th} direction
$g_o(\epsilon_s)$	Radial distribution function based on solids volume fraction
$h_{gn}(T_{rxn})$	Specific enthalpy of the n^{th} gas phase species at temperature T_{rxn}
h_{pn}	Specific enthalpy of the p^{th} phase of the n^{th} chemical species
I_{gm}	Interphase momentum transfer between gas (fluid) and solids phase m
m	(as variable) mass; (as subscript) m^{th} phase
MW	Molecular weight
MW_n	Elemental molecular weight of the n^{th} species
N_g	Number of gas species

Latin Symbols (cont.)

Term	Description
N_p	Number of chemical species in parcel p
Nu	Nusselt number
p	Pressure
P_g	Gas (fluid) pressure
P_s	Empirical pressure constant
r	Particle radius
r_{32}	Sauter mean radius
$R_{gnq}^{(k)}$	Rate of formation (destruction) of the n^{th} gas species attributed to the q^{th} reaction between the gas phase and parcel k
R_{pn}	Rate of production/consumption of the n^{th} chemical species
\mathcal{S}_{conv}	Source term for convective heat transfer
$\mathcal{S}_{gi,name}^{(k)}$	Source term for gas phase, i^{th} direction, k^{th} parcel, to support name calculation
\mathcal{S}_m	Source term for phase m
$\mathcal{S}_{mi,name}^{(k)}$	Source term for solid phase m, i^{th} direction, k^{th} parcel, to support name calculation
\mathcal{S}_p	Source term for parcel p
\mathcal{S}_{pi}	Source term for parcel p in i^{th} direction
\mathcal{S}_{rxn}	Source term for energy accompanying interphase mass transfer (chemical reaction)
\mathcal{S}_{xi}	x-interpolator function with nodal reference i
\mathcal{S}_{yj}	y-interpolator function with nodal reference j
\mathcal{S}_{zk}	z-interpolator function with nodal reference k
$\mathcal{S}_{i,j,k}$	Manufactured 3-dimensional interpolation operator at (i, j, k)
t	Time
T	Temperature
$T^{(k)}$	k^{th} parcel temperature
T_g	Gas (fluid) temperature
U_g	Gas (fluid) velocity
U_{gi}	Gas (fluid) velocity in the i^{th} direction
\bar{U}_i	Regional mean velocity in the i^{th} direction
U_m	m^{th} phase particle velocity
U_{mi}	m^{th} phase particle velocity in the i^{th} direction
$U_i^{(k)}$	k^{th} parcel velocity in the i^{th} direction

Latin Symbols (cont.)

Term	Description
$\mathcal{V}^{(k)}$	k^{th} parcel's individual particle volume
V_m	m^{th} phase particle volume
W_p	parcel statistical weight
x	General position
x_p	Center position of parcel p
X_n	Mass fraction of the n^{th} species
X_{pn}	Mass fraction of the n^{th} species, p^{th} parcel

Greek Symbols

Term	Description
α	Small constant (e.g. $1e-7$)
β	Empirical unitless exponent
$\beta_g^{(k)}$	k^{th} parcel's individual particle momentum transfer (drag) coefficient
γ	Any general cell centered variable (in context of interpolation)
γ_{cp}	Convective heat transfer coefficient
γ_p	Interpolated value of general cell centered variable, γ , to location p
$\delta x_{i+\frac{1}{2}}$	x -distance between nodes (i) and ($i + 1$)
ε_{cp}	Close-pack solids volume fraction
ε_g	Gas (fluid) volume fraction
ε_p	Restitution factor
ε_s	Solids volume fraction
λ_g	Gas (fluid) conductivity
λ_p	Interpolated value of face centered variable, λ , to location p
η	Empirical factor
ρ_m	Density of the m^{th} phase
σ	Mass weighted standard deviation of particle velocity distribution in a cell
τ	Interparticle stress (PIC model specific)
τ_D	Collision time
ϕ	Particle distribution function (general)

Acknowledgments

This work was performed in support of the U.S. Department of Energy's (DOE) Fossil Energy Crosscutting Technology Research Program. The research was executed through the National Energy Technology Laboratory's (NETL) Research and Innovation Center's Advanced Reaction Systems Field Work Proposal. Research performed by Leidos Research Support Team staff was conducted under the RSS contract 89243318CFE000003.

EXECUTIVE SUMMARY

MFiX (Multiphase Flow with Interphase eXchanges) is an open-source multiphase flow solver developed at the National Energy Technology Laboratory. Within the code, users have access to a single phase or interpenetrating continua-based multiphase two-fluid model (TFM), a discrete element model (DEM), and a particle-in-cell model (PIC). TFM, DEM, and PIC can all be used to create multiphase simulations that include hydrodynamics, chemical reactions, and heat transfer.

This document presents the underlying theory for the MFiX-PIC model only. MFiX-PIC is a Lagrangian solids model that tracks the position and trajectory of computational parcels that represent groups of identical spherical particles within a Eulerian fluid. It is firmly coupled to the fluid flow solver previously described in Musser and Carney (2020) and imitates many of the same Lagrangian methods described in Boyalakuntla (2003, 2006) and Garg et al. (2012). Evolving from 1-dimensional (Andrews and O'Rourke, 1996) and 2-dimensional (Snider et al., 1997) implementations, the current 3-dimensional PIC formulation most resembles the work of Snider (2001).

MFiX-PIC is best suited for industrial-scale, semi-dense multiphase flow simulations where trend is more important than exactness of solution. The methodology utilizes statistical averaging techniques to advance simulations quickly and carries minimal particle-level overhead. Note that solutions do appear very realistic, and verification and validation studies confirm that the methodology predicts accurate flow characteristics (Vaidheeswaran et al., 2020).

This document follows the notation and variable formats used in equations set forth in Musser and Carney (2020). It is suggested that the active reader, truly trying to digest MFiX-PIC theory, use this document in determined cooperation with Musser and Carney (2020) and Snider (2001).

1. INTRODUCTION

MFiX is a general-purpose Fortran code used to describe the hydrodynamics, heat transfer and chemical reactions in gas-solid flows. Within MFiX are three primary models: (1) the two-fluid model (TFM), (2) the discrete element model (DEM), and (3) the particle-in-cell model (PIC).

It is unlikely that every imaginable multiphase application could be equivalently simulated by these three modeling techniques. Therefore, understanding the theoretical motivation behind the models is paramount to a user selecting the most appropriate technique for their application. The theory underpinning the TFM model has been described in Musser and Carney (2020). Likewise, the theory establishing DEM has been documented in Snider (2001). And now, in this document, the theory underlying the PIC model is detailed to better inform the user of its unique advantages and disadvantages.

1.1 OVERVIEW OF MFiX-PIC

The MFiX-PIC solids model tracks the position and trajectory of computational parcels, statistical groups of particles that share the same physical characteristics (e.g. diameter and density). In the present formulation, different diameter particles of the same material must be defined as separate solid phases, each with its own statistical classification. Figure 1 illustrates this idea.

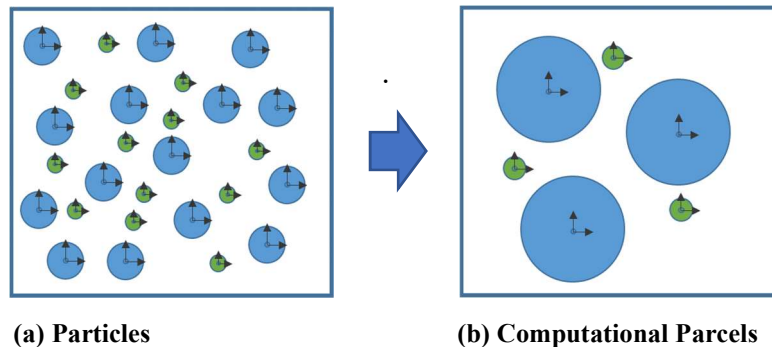


Figure 1: Visual concept of particle consolidation to computational parcels by type. (a) A single cell populated with particles. (b) The same single cell after a statistical weight has been applied to each particle type.

If one imagines that Figure 1 represents a single cell, there are 15 blue particles represented by 3 blue computational parcels, and 12 green particles represented by 3 green computational parcels. In simple terms, 1 blue parcel carries a statistical weight of 5 particles/parcel, and 1 green parcel carries a statistical weight of 4 particles/parcel.

Still thinking about Figure 1 one can immediately perceive the natural solution degradation that is inherent to this kind of statistical consolidation of particles. For example, the method must immediately lose the precise physics associated with particle-to-particle contacts and instead use more generalized representations of particle interactions. In particular, without resolving particle collisions or managing Newtonian mechanics in any way, the PIC model creates an aggregated solids stress momentum source term that affects local solids velocity directly. Snider (2001) refers to this source term as a *frictional stress model*.

The frictional stress model is driven by an evaluation of local solids volume fraction gradient and averaged field quantities. This statement implies that the model implementation is algebraic, and therefore computationally efficient. Consequently, the PIC model can deliver computational predictions for suitable large industrial applications in tractable wall time.

Aside from the frictional stress model, PIC can support subsidiary models (e.g. a collisional stress model, wall friction models) that may add to the fidelity of results. As with all coupled computational fluid dynamics (CFD) simulations, these subsidiary models will add time to the solution.

1.2 ASSUMPTIONS/LIMITATIONS

Assumptions/limitations of the MFiX-PIC model include:

- *Particles are assumed spherical in shape within computational parcels.*
Why? Subsidiary models used in the MFiX-PIC formulation pre-assume particles are spherical. Consequently, in its current implementation, MFiX-PIC should only be run with Wen-Yu, Gidaspow, Gidaspow-Blend, or Syamlal-O'Brien drag models (see Section 3.4.4 and Appendix B of Musser and Carney (2020)). Likewise, any surface area or volume dependent calculations rely on the radial (assumed sphere) definition, like chemical reactions.
- *Computational parcels must be defined by phase and maintain a mean density.*
Why? Subsidiary calculations for drag, thermal transfer, and chemical reaction rely on particle-level definitions. This allows for more simple calculations of particle diameter within each tracked parcel. For example, when density is assumed constant, and a chemical reaction takes place, a new particle diameter (within the parcel) can be calculated to reflect a mass gain/loss. Simply, accounting is easier (and faster) with this assumption.
- *Computational parcels are isothermal.*
Why? MFiX-PIC maintains no physical representation of how particles might populate a parcel. Mathematics treats each PIC parcel as a single point in space. There are no particle or parcel surfaces or other 3-dimensional physical features on which to act. In fact, the previous Figure 1 is misleading in this regard, as only the center of a PIC parcel is truly tracked. The imagined surfaces of the computational parcels are irrelevant to the mathematical model¹. Figure 2 illustrates how the mind wants to give computational parcels structure, but mathematically that structure simply does not exist.

¹ The only exception is particle-boundary interactions where an effective radius—calculated from a single particle of equivalent volume to a parcel—is used to prevent an over accumulation of parcels near domain walls. Specifically, a reflective boundary condition is applied to parcels when they are within one effective-radius of a solid boundary.

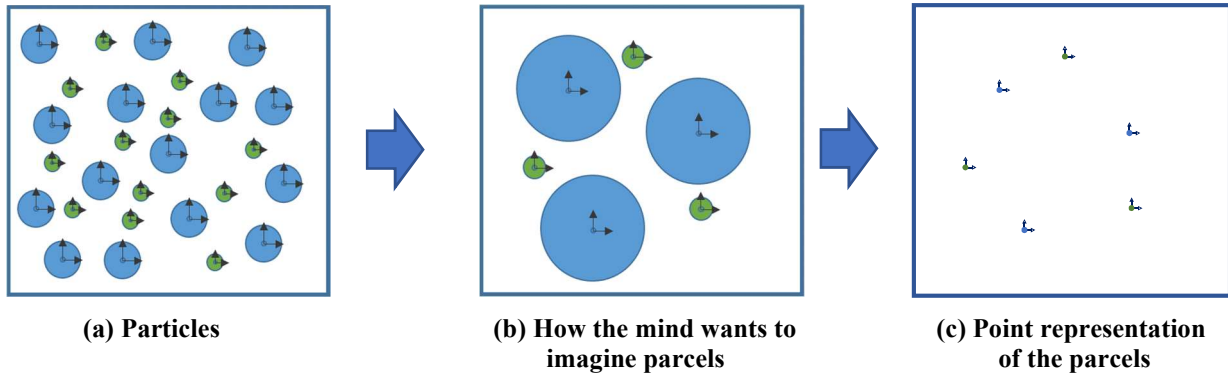


Figure 2: Computational PIC parcels are infinitesimal points in space. While the mind easily accepts consolidation of particles into “bigger” parcels, the mathematics acts only on the center of such an imagined parcel.

- Computational parcels do not experience rotation.*
Why? Figure 2 illustrates the point representation of parcels in PIC. Points cannot experience rotation.
- There are no formally modelled collisions; parcels may pass freely through each other when velocity fields warrant motion.*
Why? Figure 2 illustrates the point representation of parcels in PIC. Since no formal parcel geometry is maintained, actual surface to surface collisions cannot be calculated. A statistically driven collision model may be applied to influence solids dynamics, if needed. The user is expected to realize that choosing sensible time steps, mesh size, and statistical weights is inherent to reasonable PIC modeling.
- Computational parcels always experience adiabatic wall conditions.*
Why? Heat transfer between two touching objects requires an intrinsic knowledge of surface area. Again, Figure 2 illustrates the point representation of parcels in PIC. Surface area for heat transfer inherently does not make sense in this model.
- The PIC method is inappropriate for use in very dilute flows; a single parcel is the least amount of solids representative in any single cell, based on initial conditions.*
Why? The model requires the formation of solids fraction gradients to create estimates of changes in solids velocity. In very dilute flow (and at fully dense pack flows), the solids fraction gradients in a simulation will approach zero². When this happens, PIC may predict no solids movement (with respect to other solids) and subtle flow changes become indiscriminate. For cases that involve very dilute flow or very dense nearly close-packed flows, loss of accuracy in those areas is expected.
- Parcels interact with walls through 3-dimensional reflection.*
Why? Again, because no formal parcel geometry is maintained, and only a center point is known, a point reflection method is applied to parcels at the walls.
- The method is not formulated for 2-dimensional simulation.*
Why? Generalized PIC models can be used in 2-dimensional settings, but it was decided that application problems of interest to this development group are 3-dimensional in

² In dilute flows parcel movement is dictated by gravity, fluid-parcel interaction forces (i.e., drag), and parcel-boundary interactions. The solids stress model has little to no impact on parcel motion at low solids concentrations.

nature. Likewise, geometry input (through the MFiX graphical user interface) is provided through 3-dimensional stereolithographic CAD file (STL) files. Hence no 2-dimensional computational support was built into the MFiX-PIC model. Note, however, that 2-dimensional problems can be “faked” in MFiX-PIC by building simulations that are a minimum of 3 cells wide in the non-modeled direction. The 3-cell restriction is related to interpolation techniques inherent to the method.

1.2.1 **General Recommendation**

Understanding that PIC parcels are completely mathematical in nature, it is most acceptable to visualize particle distributions in MFiX-PIC results using volume fraction fields, and not individual renderings of parcels. Note that some users may prefer the “particle-like” outputs created through MFiX’s Visual ToolKit (VTK) output formats. The user must be careful to note that depending on how statistical weights have been applied, and what kind of computational mesh was chosen, a Lagrangian depiction of results may *look* weird (see assumptions), but still be correct. For example, edges of imagined parcels may live outside of boundaries or may indiscriminately overlap. This is normal.

1.3 DOCUMENT ORGANIZATION

MFiX-PIC simulations utilize a Eulerian fluid phase model coupled to a Lagrangian solids phase model. The fluid phase model is identical to that described in Chapter 2 of Musser and Carney (2020). Its description will not be repeated here.

Section 2 presents the theoretical Lagrangian solids phase model.

Section 3 presents numerical details unique to MFiX-PIC.

2. LAGRANGIAN SOLIDS PHASE MODEL UTILIZED IN PIC

2.1 OVERVIEW

This section presents the MFiX Lagrangian solids phase model. While TFM may interpret solids as liquid droplets or gas bubbles, this is NOT true in PIC. The solids phase in PIC modeling is decidedly solid particles that are statistically managed as computational parcels.

Historically, in Snider et al. (1997) and Snider (2001), PIC models are derived from a Liouville equation describing the time evolution of a particle distribution function, $\phi(x, U_m, \rho_m, V_m, t)$, where x is particle position, U_m is particle velocity, ρ_m is particle density, V_m is particle volume, and t is time. The subscript m is indicative of other MFiX documentation, nodding to solids phase m , which in this case would indicate a unique solids class of particles.

$$\frac{d\phi}{dt} + \nabla \cdot (\phi U_m) + \nabla_{U_m} \cdot (\phi A_m) = 0 \quad (1)$$

Here ∇_{U_m} is the divergence operator with respect to the velocity, U_m and A_m is the discrete particle phase acceleration.

The particle distribution function integrated over velocity and mass will yield the likely number of particles per unit volume at the position, x , at time, t , for small intervals of $(V_m + dV_m, \rho_m + d\rho_m, U_m + dU_m)$. The solids volume fraction, ε_s , can then be represented through the distribution function using a volume integral.

$$\varepsilon_s = \iiint \phi V_m dV_m d\rho_m dU_m \quad (2)$$

The solids phase is coupled to the Eulerian governing equations through the interphase momentum transfer term. This can be found in Musser and Carney (2020) under Section 3.4.4. Allowing I_{gm} to be the contribution due to interphase momentum transfer between the gas and the m^{th} solid phase,

$$I_{gm} = \iiint \phi V_m \rho_m \left[D_m (U_g - U_m) - \frac{1}{\rho_m} \nabla p \right] dV_m d\rho_m dU_m \quad (3)$$

where D_m is drag coefficient and ∇p is pressure gradient. In practice, the interphase momentum is adjusted by weighting factors associated with the distribution function, but the above is presented in theoretical notation, not as discrete implementation. Discrete management is discussed in later sections.

2.2 CONSERVATION EQUATIONS

Throughout this section, the word *particle* indicates what the reader might expect, a single piece of material, spherical in nature, having physical characteristics that can be uniquely defined (like density, chemical composition, etc.); the word *parcel* indicates a statistical collection of particles of similar physical characteristics.

This section presents the MFiX-PIC governing equations which are solved for each parcel in the system.

2.2.1 Conservation of Mass

The conservation of mass (or continuity equation) for the p^{th} MFiX-PIC parcel is given by managing the particle's statistical weight, W_p , and considering its mass change, $\frac{dm}{dt}$, under the effects of chemical reaction.

$$\frac{d}{dt}(W_p m_p) = W_p \sum_{n=1}^{N_p} R_{pn} \quad (4)$$

where R_{pn} is the rate of production/consumption of the n^{th} chemical species, and N_p is the number of chemical species. This is not unlike the conservation of mass equation defined in Musser and Carney (2020) as Equation 3-1, except for statistical weight notation, necessary for the nature of PIC.

Specifically, the right-hand side of (4) accounts for interphase mass transfer because of heterogenous chemical reactions or physical processes, like evaporation. In non-chemically reactive simulations (or those without phase change), the right side of Equation (4) equals zero.

Note how the statistical weight acts as a multiplier to a simple calculation made at particle level.³ In this way, MFiX-PIC can leverage particle-level subroutines developed for MFiX-DEM without duplicating programmatic overhead. This same management of W_p will appear in many descriptions throughout this document.

2.2.2 Conservation of Species Mass

The n^{th} species mass conservation equation for the p^{th} MFiX-PIC parcel is given by

$$\frac{d}{dt}(W_p m_p X_{pn}) = W_p R_{pn} \quad (5)$$

where X_{pn} is the n^{th} chemical species mass fraction, and R_{pn} is the rate of formation of species mass attributed to chemical reactions or physical processes. In non-chemically reactive simulations (or those without phase change), the right side of Equation (5) equals zero.

Note how the parcel's statistical weight, W_p , acts as a multiplier to a calculation made at particle level. This indicates that MFiX is once again leveraging MFiX-DEM subroutines.

2.2.3 Conservation of Translational Momentum

The general conservation of translation momentum for the p^{th} MFiX-PIC parcel in the i^{th} coordinate direction is given by

³ The MFiX-PIC implementation tracks particle data – not parcel data. As a result, extrinsic properties like mass and volume must be scaled by the parcel weighting factor to obtain the correct value. For example, the volume of a particle is multiplied by the weighting factor to evaluate the Eulerian solids volume fraction.

$$W_p m_p \frac{dU_i}{dt} = W_p \left(m_p g_i + \frac{m_p}{\varepsilon_s \rho_s} \nabla_{\vec{x}} \tau_p \right) \quad (6)$$

where U_i is the parcel velocity, and g_i is the gravity body force. The first term on the right-hand side is the gravitational body force. The second term is a PIC-specific term derived from interparticle stress, τ , described in detail in the section Interparticle Stress below.

As expected, the position of a parcel is related to its velocity through

$$\frac{dx_i}{dt} = U_i \quad (7)$$

where x_i is the parcel position in the i^{th} coordinate direction.

Interparticle Stress

The interparticle stress variable, τ , follows the form suggested by Snider (2001). Specifically,

$$\tau = \frac{P_s \varepsilon_s^\beta}{\max(\varepsilon_{cp} - \varepsilon_s, \alpha(1 - \varepsilon_s))} \quad (8)$$

where ε_{cp} indicates a pre-determined, problem-specific, close-pack volume fraction for the solids phase. P_s is an empirical pressure constant relatable to the scale and unit of the problem under evaluation, and β is an empirical unitless exponent, usually between 2 and 5. α is a tiny constant (e.g. 1e-7) to assure a non-zero denominator in calculations. Note that the form of the interparticle stress term as well as some literary suggestions (CPFD Software, LLC, 2016) for the values of P_s and β come directly from the work of Auzeais et al. (1988), where they show ε_{cp} is upper-limited to the value 0.64, and the values of P_s and β are chosen to best align with their particle settling experimental data. Thus, for prudent simulation, an array of values for P_s and β must be investigated and aligned to some experimental dataset before legitimate value is placed on predictive computational results using PIC.

2.2.4 Conservation of Internal Energy

The general conservation of internal energy for the p^{th} MFiX-PIC parcel follows the same theoretical underpinnings as DEM. The internal energy is presented in terms of temperature. For an isothermal parcel (a PIC assumption),

$$W_p m_p C_p \frac{dT}{dt} = -W_p \left(\sum_{n=1}^{N_p} h_{pn} R_{pn} \right) + \mathcal{S}_p \quad (9)$$

where C_p and T are parcel specific heat and temperature (same as particle values). The first term on the right-hand side represents changes in internal energy accompanying species formation or destruction from chemical reaction and/or phase change (h_{pn} is the n^{th} species specific enthalpy). The last term, \mathcal{S}_p , is a general source term. Note that \mathcal{S}_p might represent particle-

particle heat transfer (currently 0 in PIC; there is no conduction model), fluid particle heat transfer (convection) or radiative heat transfer (currently 0 in PIC; radiation model is pending).

2.3 PARTICLE-PARTICLE MOMENTUM TRANSFER

There is no particle-particle momentum transfer modeled in MFiX-PIC. Instead, there is a collision damping model that can be optionally applied. Otherwise, in general, PIC modeling assumes the free passage of particles through one another.

2.3.1 Optional Collisional Damping

To account for interaction between particles internal to a parcel, an optional collision damping model can be employed. This term would appear as an additional source term, \mathcal{S}_{pi} in the conservation equation for parcel translational momentum. In the basic model, $\mathcal{S}_{pi} = 0$, by default. However, when including the effect of collisional damping, O'Rourke and Snider (2009, 2010) describes a new term related to the particle distribution, ϕ , and how it can be re-imagined in terms of a collision time, τ_D , and the relationship between a parcel's local velocity, U_i and a cell or region mean velocity, \bar{U}_i .

$$\mathcal{S}_{pi} \approx \frac{1}{2\tau_D} \frac{\partial}{\partial U_i} [\phi(U_i - \bar{U}_i)] \quad (10)$$

In practice, τ_D is empirically calculated, and \mathcal{S}_{pi} is applied as an incremental mass weighted acceleration. Specifically,

$$\frac{1}{\tau_D} = \frac{16}{\sqrt{3\pi}} \frac{\varepsilon_s \sigma}{r_{32}} g_o(\varepsilon_s) \eta (1 - \eta) \quad (11)$$

where σ is the mass-weighted standard deviation of the parcel velocity distribution in a cell, r_{32} is the Sauter mean radius of the particles in that same cell, $g_o(\varepsilon_s)$ is a radial distribution function based on solids volume fraction, ε_s , and $\eta = \frac{1+e_p}{2}$ where e_p is a user-supplied restitution coefficient.

In practice, the radial distribution function is represented as:

$$g_o(\varepsilon_s) = \frac{\varepsilon_{cp}}{\varepsilon_{cp} - \varepsilon_s} \quad (12)$$

And \mathcal{S}_{pi} is

$$\mathcal{S}_{pi} = \frac{1}{2\tau_D} (U_i - \bar{U}_i) \quad (13)$$

This implies that a small acceleration or deceleration is applied to imitate collision action. O'Rourke and Snider (2010) indicates that the application of collision damping is entirely empirical and results should be matched to experiment, if possible.

2.4 FLUID-PARCEL MOMENTUM TRANSFER

By default, MFiX accounts for gas-solids buoyancy through a shared gas-pressure formulation termed Model-A (Musser and Carney, 2020). As such, the fluid-parcel drag force acting on a parcel k is given by:

$$\mathcal{S}_{mi,drag}^{(k)} = W_k \left(-\frac{dP_g}{dx_i} \mathcal{V}^{(k)} + \beta_g^{(k)} \mathcal{V}^{(k)} (U_{gi} - U_i^{(k)}) \right) \quad (14)$$

where $\mathcal{V}^{(k)}$ is the k^{th} parcel's single particle volume, $\beta_g^{(k)}$ is the k^{th} parcel's particle momentum transfer (a.k.a. drag) coefficient, and P_g and U_{gi} are the fluid phase pressure and velocity, respectively. The entire expression is then modified by the statistical weight, W_k , assigned to parcel k . The drag force is added to the translational momentum equation through the general source term, \mathcal{S}_{pi} . Similarly, the fluid phase momentum source is

$$\mathcal{S}_{gi,drag} = W_k \left(\sum_k \frac{dP_g}{dx_i} \mathcal{V}^{(k)} + \beta_g^{(k)} \mathcal{V}^{(k)} (U_i^{(k)} - U_{gi}) \right) \quad (15)$$

which is added to the fluid phase momentum equation through its general source term. Special consideration is needed when relating quantities (e.g., gas velocity and drag force) between the fluid and particles. See MFiX Documentation (Garg et al., 2012).

2.5 PARCEL-PARCEL HEAT TRANSFER

A geometrically supported value for direct contact conduction is intractable for the MFiX-PIC model. Specific particle position within a parcel is unknown, so the geometric surface areas and contact positions needed for conduction computations are not calculable.

2.6 RADIATIVE HEAT TRANSFER

Currently MFiX-PIC does not support radiative heat transfer.

2.7 FLUID-PARCEL CONVECTIVE HEAT TRANSFER

Convective heat transfer between parcel (k) and the fluid is given by

$$\mathcal{S}_{conv} = W_k \left(\gamma_{cp} A_s (T_g^{(k)} - T^{(k)}) \right) \quad (16)$$

where W_k is the statistical weighting function assigned to parcel k , γ_{cp} is the convective heat transfer coefficient, and A_s is the particle surface area. $T^{(k)}$ is parcel temperature (which is equivalent to particle temperature by assumption) and T_g is the fluid phase temperature.

γ_{cp} is commonly modeled by the Nusselt number,

$$\gamma_{cp} = \frac{\lambda_g}{2r} \text{Nu} \quad (17)$$

where r is the particle radius, and λ_g is the fluid thermal conductivity. Heat transfer from convection is added to the solids internal energy equation through a general source term.

Likewise, the heat transfer from convection is added to the gas-phase internal energy equation through the general source term (Musser and Carney, 2020).

2.8 ENERGY TRANSFER ACCOMPANYING MASS TRANSFER

Energy transfer accompanying interphase mass transfer between parcel (k) and the fluid is given by:

$$\mathcal{S}_{rxn} = W_k \sum_p \sum_{n=1}^{N_g} h_{gn}(T_{rxn}) R_{gnq}^{(k)} \quad (18)$$

$R_{gnq}^{(k)}$ is the rate of formation (or destruction) of the n^{th} gas phase species attributed to the q^{th} reaction between the gas phase and parcel (k). $h_{gn}(T_{rxn})$ is the specific enthalpy of the n^{th} gas phase species at temperature, T_{rxn} , identified by:

$$T_{rxn} = \begin{cases} T_g & \text{for } R_{gnq}^{(k)} \leq 0 \text{ (i.e., consumption of } n^{th} \text{ gas species)} \\ T^{(k)} & \text{for } R_{gnq}^{(k)} > 0 \text{ (i.e., formation of } n^{th} \text{ gas species)} \end{cases} \quad (19)$$

where T_g and $T^{(k)}$ are the gas and parcel temperatures, respectively. Energy transfer accompanying interphase mass transfer is subtracted from the solids internal energy equation through the general source term.

Similarly, the heat transfer from fluid-phase energy is added to the gas-phase internal energy equation through the general source term (Musser and Carney, 2020).

2.9 PARCEL PHYSICAL PROPERTIES

Parcel properties are natural extensions of particle properties since the PIC assumption is that parcels are made up of uniform groupings of particles, all sharing the same physical properties. So, in the case of mixture molecular weight and mixture specific heat, particle and parcel properties are identical.

2.9.1 Mixture Molecular Weight

The particle mixture molecular weight, MW, is either specified as constant or calculated as

$$\frac{1}{MW} = \sum_{n=1}^N \frac{X_n}{MW_n} \quad (20)$$

where X_n and MW_n are the mass fraction and elemental molecular weight of the particle n^{th} chemical species.

2.9.2 Mixture Specific Heat

The particle mixture specific heat, C_p , is either specified as constant or calculated as

$$C_p = \sum_{n=1}^N X_n C_{pn} \quad (21)$$

where C_{pn} is the specific heat of the particle n^{th} chemical species.

3. NUMERICAL DETAILS UNIQUE TO MFiX-PIC

3.1 OVERVIEW

This section explains how data is manipulated between the Eulerian grid and Lagrangian parcels.

3.2 BI-LINEAR INTERPOLATION

Values between Eulerian cell centers, face cell centers, and parcel position are managed through interpolation operators. To accomplish this in MFiX-PIC, bi-linear operators are combined in each axial direction. Using the notation of Snider et al. (1997), a 3-dimensional interpolation operator is formed as:

$$S_{i,j,k} = S_{xi}S_{yj}S_{zk} \quad (22)$$

Figure 3 shows the x-interpolation function, S_{xi} . By inspection, one can see a hat function valued at 1 at the X-node i that decreases linearly to 0 at its neighboring $(i-1)$ and $(i+1)$ nodes. This occurs while Y and Z nodes (j and k) are held constant. Similar functions are used in the y- and z-directions, allowing the user to apply the correct nodal weight to variables in off-node locations.

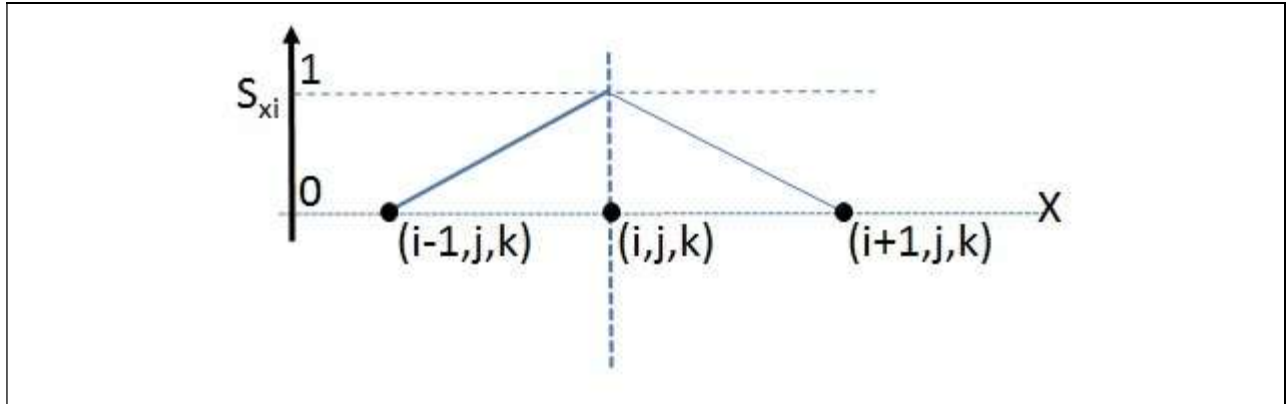


Figure 3: Typical Bi-linear Interpolation Operator, S_{xi} .

From an arithmetic perspective,

$$S_{xi} = \frac{(x_{i+1} - x_p)}{\delta x_{i+1/2}} \quad (23)$$

where x_p is the x-center position of the parcel, and $\delta x_{i+1/2} = x_{i+1} - x_i$, the distance between adjacent cell-centers that bound x_p (i.e. $x_p \in (x_i, x_{i+1})$). Allowing a general parcel position to be considered as the vector $\vec{x}_p = \langle x_p, y_p, z_p \rangle$, likewise, values for S_{yj} and S_{zk} are formed.

3.2.1 Grid to Parcel Management

In 3-dimensions, interpolation operators may be difficult to visualize. A parcel center (shown as a star in Figure 4) is located within a 3-dimensional block made of the 8 closest centers of surrounding cells. Each center-held variable contributes value to the parcel location (at star) in a summative way, with each weight coming from a local value of the interpolation operator.

For the figure shown, and for a general cell-centered variable, γ , one can quickly write down that at center-parcel location p , the value of γ_p is calculated as:

$$\begin{aligned} \gamma_p = & S_{i,j,k}\gamma_{i,j,k} + S_{i,j+1,k}\gamma_{i,j+1,k} + S_{i,j,k+1}\gamma_{i,j,k+1} + S_{i,j+1,k+1}\gamma_{i,j+1,k+1} \\ & + S_{i+1,j,k}\gamma_{i+1,j,k} + S_{i+1,j+1,k}\gamma_{i+1,j+1,k} + S_{i+1,j,k+1}\gamma_{i+1,j,k+1} \\ & + S_{i+1,j+1,k+1}\gamma_{i+1,j+1,k+1} \end{aligned} \quad (24)$$

The key is simply location awareness and forming suitable cell-centered blocks around the centers of parcels for the variables required.

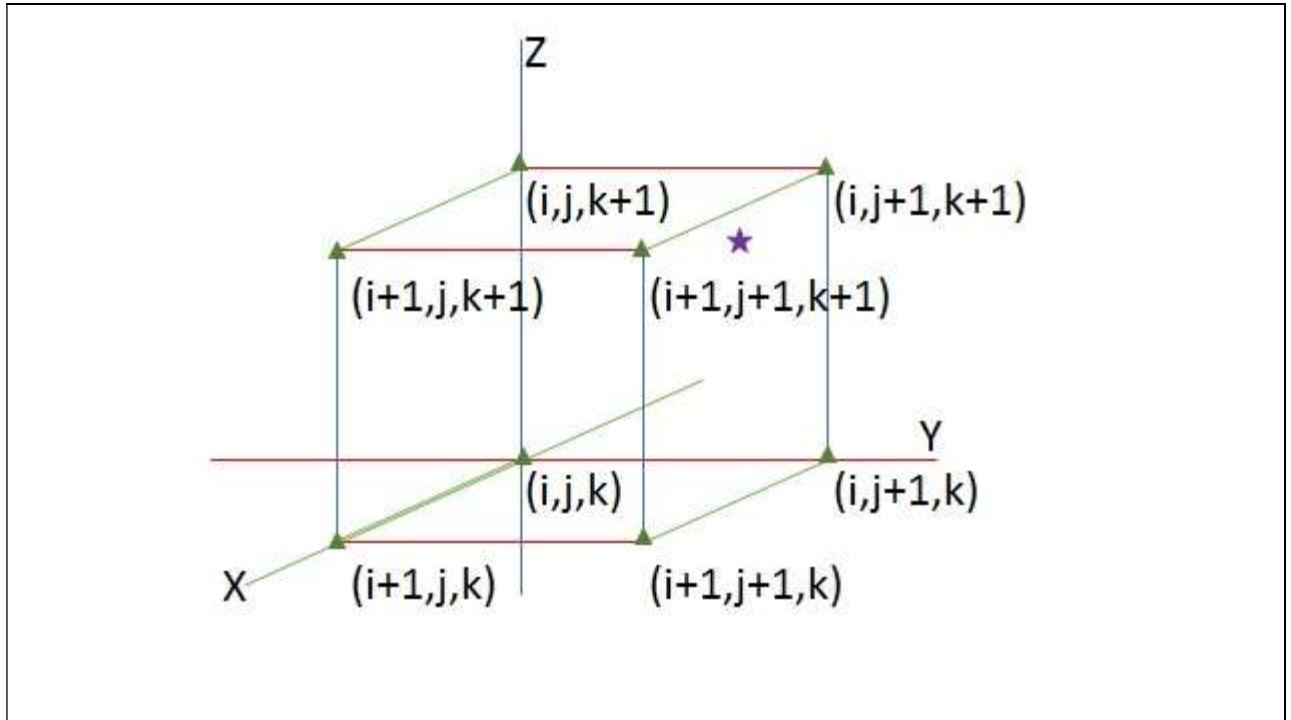


Figure 4: Parcel (star) in 3-dimensional cell-center view (triangles) used for interpolation.

The evaluation of gradient is also necessary at parcel locations. Following the calculus of the Eulerian property, γ , as shown in relation to Figure 3, and interpolated to the parcel position, p , an associate gradient is easily derived:

$$\begin{aligned} \nabla \gamma_p = \nabla (& S_{i,j,k} \gamma_{i,j,k} + S_{i,j+1,k} \gamma_{i,j+1,k} + S_{i,j,k+1} \gamma_{i,j,k+1} + S_{i,j+1,k+1} \gamma_{i,j+1,k+1} \\ & + S_{i+1,j,k} \gamma_{i+1,j,k} + S_{i+1,j+1,k} \gamma_{i+1,j+1,k} + S_{i+1,j,k+1} \gamma_{i+1,j,k+1} \\ & + S_{i+1,j+1,k+1} \gamma_{i+1,j+1,k+1}) \end{aligned} \quad (25)$$

$$\nabla \gamma_p = \sum_m \gamma_m \nabla S_m \quad (26)$$

where m represents appropriately identified Eulerian nodes, as previously described as cell-centered blocks around the centers of parcels for the gradient of variables required.

Finally, value exchange between Eulerian face centers and parcel positions is similarly accomplished. One merely slides the box view shown in Figure 4 to a face-centered position that is appropriate for the variable in question. Figure 5 illustrates an appropriate boxing for values stored on the xz -faces (e.g. y -velocity).

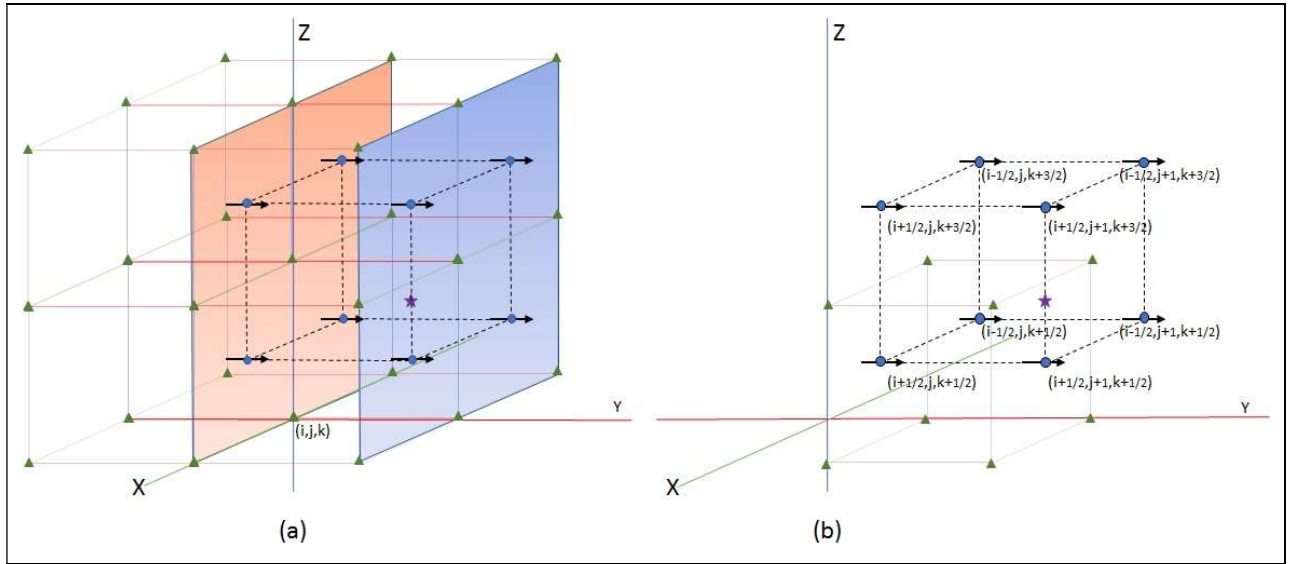


Figure 5: (a) An extension of Figure 4, showing velocity stored at xz -face centers (circles) in the original context of cell-center nodes (triangles). (b) Pulling the new face-centered box out of (a) and applying labels while maintaining the original cell center view of Figure 4.

From this perspective, data stored on cell-faces interpolates to parcel positions under a similar blocking scheme to cell-center values. For a general xz -face-centered variable, λ , one can quickly write down that at center-parcel location p , the value of λ_p is calculated as:

$$\begin{aligned}
 \lambda_p = & S_{i+\frac{1}{2},j,k+\frac{1}{2}} \lambda_{i+\frac{1}{2},j,k+\frac{1}{2}} + S_{i+\frac{1}{2},j+1,k+\frac{1}{2}} \lambda_{i+\frac{1}{2},j+1,k+\frac{1}{2}} + S_{i+\frac{1}{2},j,k+\frac{3}{2}} \lambda_{i+\frac{1}{2},j,k+\frac{3}{2}} \\
 & + S_{i+\frac{1}{2},j+1,k+\frac{3}{2}} \lambda_{i+\frac{1}{2},j+1,k+\frac{3}{2}} + S_{i-\frac{1}{2},j,k+\frac{1}{2}} \lambda_{i-\frac{1}{2},j,k+\frac{1}{2}} \\
 & + S_{i-\frac{1}{2},j+1,k+\frac{1}{2}} \lambda_{i-\frac{1}{2},j+1,k+\frac{1}{2}} + S_{i-\frac{1}{2},j,k+\frac{3}{2}} \lambda_{i-\frac{1}{2},j,k+\frac{3}{2}} \\
 & + S_{i-\frac{1}{2},j+1,k+\frac{3}{2}} \lambda_{i-\frac{1}{2},j+1,k+\frac{3}{2}}
 \end{aligned} \tag{27}$$

Again, the key to proper formulation is location awareness, and forming suitable calculation blocks around each parcel. Note that xy- and yz- face centered values will have a different basis of interpolation operators than what is shown here for xz.

Higher order interpolation methodologies do exist. However, for evaluating dense particle flows, the simple bi-linear method presented here appears adequate and is computationally inexpensive for large datasets.

3.2.2 Parcel to Grid Management

The only Lagrange value maintained at the parcel location, and indirectly required by the Eulerian grid is the parcel center location itself. The location implicitly translates to a solids volume fraction by an evaluation of the number of parcels in any given cell. Arithmetically,

$$\varepsilon_{s_{i,j,k}} = \frac{1}{V_{i,j,k}} \sum_p^{N_p} W_p V_p S_{i,j,k} \tag{28}$$

Where $V_{i,j,k} = \delta x_i \delta y_j \delta z_k = (x_{i+1/2} - x_{i-1/2})(y_{j+1/2} - y_{j-1/2})(z_{k+1/2} - z_{k-1/2})$ is the volume of the Eulerian cell, N_p is the number of parcels in that Eulerian cell, W_p is the number of particles in a given parcel and V_p is the volume of particles in the given parcel.

3.3 BOUNDARY MANAGEMENT

Application problems often introduce a physical boundary defined by the intersection of the Eulerian grid with a STL. It is common for the STL to be made up of many small triangular surfaces, knitted together to form what appears to the user as a smooth surfaced object. If the user focuses on a single cell where the STL intersects the computational grid, and names this a boundary cell, a close inspection may reveal multiple facets of the STL within that same cell. From this single observation, it is easy to extrapolate that boundary cells are often geometrically unique. Hence, each boundary cell is managed algorithmically to better characterize fluid/particle/boundary interaction in these unique locations.

First, because MFiX-PIC modeling is highly dependent on interpolation and gradients, the MFiX code imposes boundary cell solids pressure values in a way to maintain a zero gradient between the cells that are interior to the calculation domain and the boundary itself. Likewise, boundary cells are managed so that they do not improperly weight interpolated values at parcel locations. In this way, the boundary does not influence the solids stress model as defined by Equation 8 and is masked through the bi-linear interpolation method already described. Without this assumption,

the bi-linear interpolation method applied to cells near a boundary would create errant values, often causing unexpected and non-physical particle behavior in boundary cells.

Furthermore, as a particle/parcel is moved discretely through the MFiX-PIC algorithm, it is possible for it to move *through* a boundary during a solids time step. Obviously, this is not a physical possibility, so a sweep of particle/parcel locations along boundary cells is completed before a time step is considered complete. When a particle/parcel is identified on the *outside* of a boundary, several evaluations are made. First, if a particle/parcel is located outside of the fluid domain (i.e. the parcel moved into a grid location where fluid calculations are not performed), a local search is executed to determine if a valid computational cell is available in which to relocate. If a valid fluid cell is not identified, the particle/parcel is deleted, and a small mass error is accrued. Next, a sweep over local STL facets is made to determine if a boundary wall was penetrated. The results of a ray-triangle-intersection detection algorithm and closest-point-to-triangle algorithm are used to identify any facet(s) the particle/parcel may have penetrated. Finally, the normal vectors from penetrated facets are used to evaluate the most likely boundary penetration points, and direct modification of the particle/parcel location is made through reflection.

This is different from DEM models where a Newtonian interaction with boundaries is discretely calculated. In PIC, for speed, this level of resolution is ignored, and instead, the particle/parcel is placed back inside the computational domain, using its effective radius and reflection direction as a guide for placement.

4. CONCLUDING REMARKS

A PIC method was added to MFiX. Application is suggested for large-scale devices where the DEM method would prove intractable.

5. REFERENCES

- Andrews, M.; O'Rourke, P. The multiphase particle-in-cell (MP-PIC) method for dense particle flow. *International Journal of Multiphase Flow* **1996**, *22*, 379–402.
- Auzerais, F.; Jackson, R.; Russel, W. The resolution of shocks and the effects of compressible sediments in transient settling. *Journal of Fluid Mechanics* **1988**, *195*, 437–462.
- Boyalakuntla, D. Simulation of granular and gas-solid flows using discrete element method. PhD Thesis, Carnegie Mellon University, Pittsburgh, 2003.
- Boyalakuntla, D.; Pannala, S. Summary of Discrete Element Model (DEM) implementation in MFiX; Morgantown, December 2006. <http://www.mfix.org/documents/MFiXDEM2006-4-1.pdf>
- CPFD Software, LLC. Barracuda Virtual Reactor User Manual, Release 17.0.5. Aug 31, 2016. <https://www.scribd.com/document/397798708/Barracuda-User-Manual>.
- Garg, R.; Galvin, J.; Li, T.; Pannala, S. Documentation of open-source MFiX-DEM software for gas-solids flows; 2012. https://mfix.netl.doe.gov/documentation/dem_doc_2012-1.pdf
- Musser, J.; Carney, J. *Theoretical Review of the MFiX Fluid and Two-Fluid Models*; NETL Technical Report Series; U.S. Department of Energy, National Energy Technology Laboratory: Morgantown, WV, 2020, p. 96.
- Musser, J.; Syamlal, M.; Shahnam, M.; Huckaby, D. E. Constitutive equation for heat transfer caused by mass transfer. *Chemical Engineering Science* **2015**, *123*, 436–443.
- O'Rourke, P.; Snider, D. An improved collision damping time for MP-PIC calculations of dense particle flows with applications to polydisperse sedimenting beds and colliding particle jets. *Chemical Engineering Science* **2010**, *65*, 6014–6028.
- O'Rourke, P.; Snider, D. A model for collisional exchange in gas/liquid/solid fluidized beds. *Chemical Engineering Science* **2009**, *64*, 1784–1797.
- Snider, D. M. Three-Dimensional Multiphase Particle-in-Cell Model for Dense Particle Flows. *Journal of Computational Physics* **2001**, *170*, 523–549.
- Snider, D.; O'Rourke, P.; Andrews, M. *An Incompressible Two-Dimensional Multiphase Particle-In-Cell Model for Dense Particle Stress*; Los Alamos National Laboratory, Los Alamos, June 1997.
- Vaidheeswaran, A.; Musser, J.; Clarke, M. *Verification and Validation of MFiX-PIC*; NETL Technical Report Series; U.S. Department of Energy, National Energy Technology Laboratory, Morgantown, WV, 2020, p.48. DOI: 10.18141.1593276.

This page intentionally left blank.



Brian Anderson, Ph.D.

Director
National Energy Technology Laboratory
U.S. Department of Energy

John Wimer

Associate Director
Strategic Planning
Science & Technology Strategic Plans
& Programs
National Energy Technology Laboratory
U.S. Department of Energy

Bryan Morreale

Executive Director
Research & Innovation Center
National Energy Technology Laboratory
U.S. Department of Energy